Università degli Studi di Roma
"Tor Vergata"

Industrial Engineering Department

Bachelor degree of Engineering Sciences

Deposition and X-RAY Characterization of Oxide Thin Films for Green Energy Application

Nikolas Vitaliti

supervised by
Prof. Simone Sanna

Academic year: 2022/23

Abstract

This report reviews newly developed miniaturized systems for energy conversion and storage.
Growing demand on thin film technology has prompted extensive research in the development of devices able to harvest and storage energy. Among them we can find solar cells, batteries, super capacitors and fuel cells that are poised to revolutionize the energy economy of our world. Modern society runs on the energy that fossil fuels posses, dependence that is not sustainable due to several factors.

This new promising science shows properties that can be very different from that of their corresponding bulk structure.
For instance, a reduction to the micro-scale of the fuel cell component's thickness leads to great performances increase due to a working temperature reduction of about 350°C.

Thin film fabrications are generally carried out by depositing the required material atom by atom over a previously deposited substrate.

The deposition of both the former and the latter have been carried out by Pulsed Laser Deposition. PLD is an excellent and simple film growth technique, able to accurately reproduce the target composition onto the substrate.

The crystalline quality and the morphological structure of the samples have been investigated and analyzed with various techniques.

Contents

Fuel cells

1.1 Overview

Fuel cells have several benefits and applications, mostly in combustion-based technologies like power plants or vehicles, because they are able to convert energy with a lower to zero emission and an higher efficiency (exceeding 60%). [5] [17]

Fuel cells efficiently and cleanly produce electricity through a chemical reaction between Oxygen and Hydrogen (or other fuels) where the byproducts are water and heat.
A schematic representation of a fuel cell is reported in Fig. 1.1.

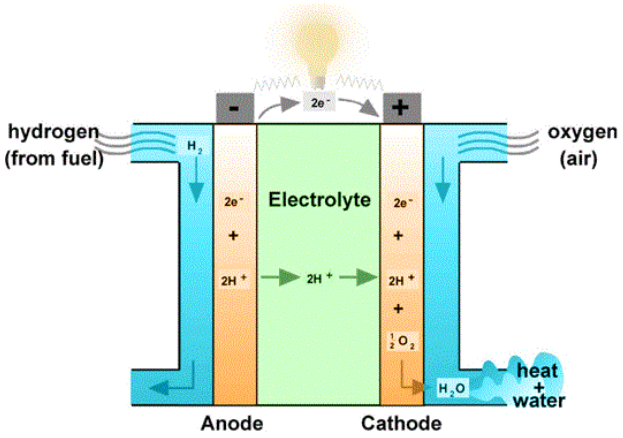

Figure 1.1: Construction and working of a Solid oxide fuel cell [27]

In a typical fuel cell, gaseous fuels are fed continuously to the anode (negative electrode) and an oxidant (i.e. oxygen from air) is fed continuously to the cathode (positive electrode).

The electrochemical reaction takes place at the electrodes to produce an electric current. These chemical reactions can be expressed as follows:

Anode reaction: $2H_2 + 2O^{2-} \rightarrow 2H_2O + 4e^-$

Cathode reaction: $O_2 + 4e^- \rightarrow 2O^{2-}$

Overall cell reaction: $2H_2 + O_2 \rightarrow 2H_2O$

1.2 Solid Oxide Fuel Cells (SOFCs)

Solid oxide fuel cells (SOFCs) offer a clean, pollution-free technology capable of electrochemically generate electricity at high efficiencies. [26]
State-of-the-art SOFCs offer many advantages that can be briefly summarized as follows:

- Flexibility in the fuel choice. SOFC systems can run on fuels other than pure hydrogen gas. However, hydrogen has to be present in the chosen fuel as it necessary for the reactions listed in the previous section.
- High electrical efficiency of around 60 %
- Usable byproducts. The high temperature exhaust gas can be utilized for additional power generation in a combined-cycle application i.e. Rankine or Brayton. [2]
- No presence of noble metals, which implies lower costs.
- Extremely low emissions. By eliminating the danger of carbon monoxide in exhaust gases: CO produced is converted in CO_2 at high operating temperatures. [33]

The largest disadvantage instead is the high operating temperature, which results in longer start-up times and mechanical and chemical compatibility issues.

1.3 Micro-SOFCs

In the past decades, materials used to build SOFCs were usually bulky ceramics and thick films (In the order of micrometers).
However, state-of-the-art micro-SOFCs use ion-conducting ceramic electrolytes with a thickness ranging in the nanometers scale [1]. This improvement decreased the operating temperature from 800-1000°C to 600-800°, without decreasing the cell performance.

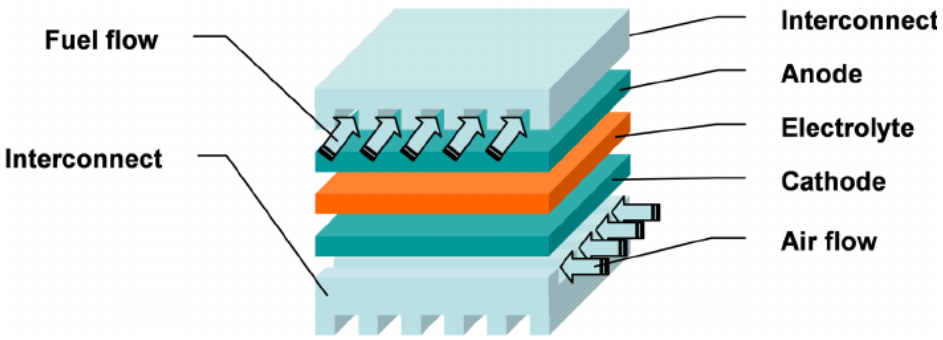

Figure 1.2: Different components constituting a planar μ-SOFC [19]

These lower operating temperatures enable the use of lower-cost metallic inter-connectors (used to stack fuel cells and increase the energy output) and reduce the thermal stress to which they are subjected.
Furthermore, they possibly allow their use as portable power generators in devices such as laptop computers and mobile telephones. Fig. 1.2 shows the schematic of a planar micro-SOFC, although they can also be constructed with tubular shapes.

1.4 Solid Oxide Electrolysis Cells (SOECs)

Solid Oxide Electrolysis Cells are the leading technology for a green production of hydrogen. The general functioning is the opposite of the one of a SOFC, namely the SOEC uses electricity to split water (H_2O) into hydrogen (H_2) and oxygen (O_2).
This is a very compelling result, as the hydrogen is a clean fuel that can be easily stored. The actual reactions occurring at the anode and the cathode, along with an overview of the net reaction is therefore given below: [20]

Anode reaction: $2O^{2-} \rightarrow O_2 + 4e^-$

Cathode reaction: $H_2O + 2e^- \rightarrow H_2 + O^{2-}$

Overall cell reaction: $2H_2O \rightarrow 2H_2 + O_2$

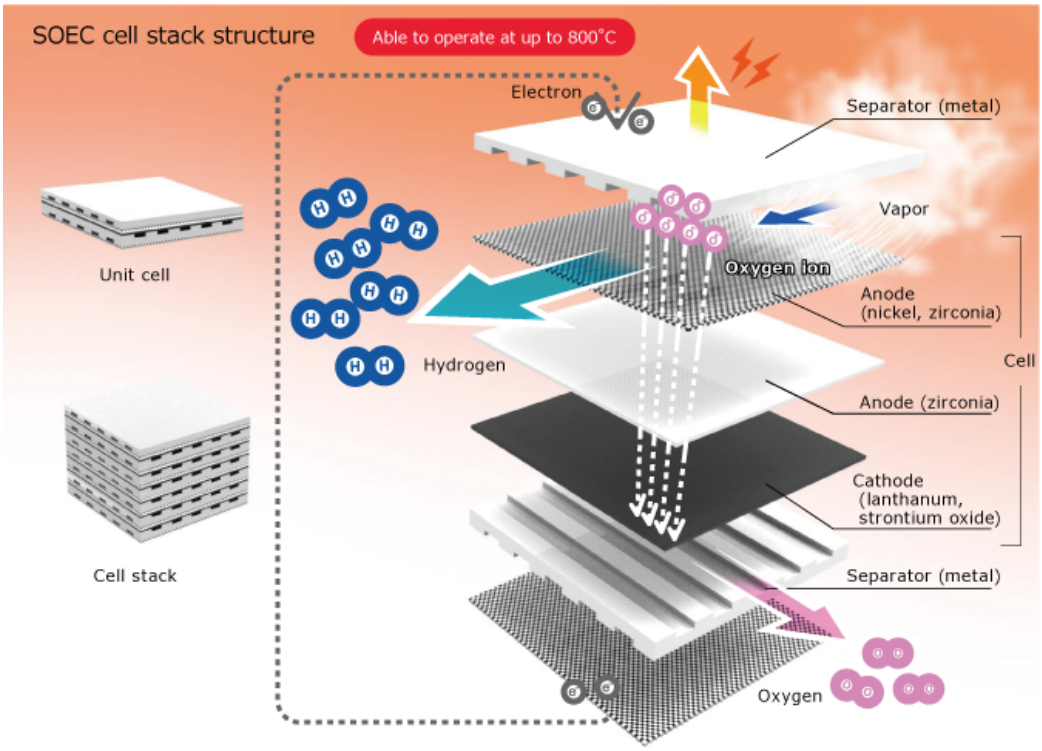

Figure 1.3: Unit and cell SOEC structures and characteristics.[28]

Materials used for the research

2.1 Complex Oxides

Complex oxides are solid-state components essential for the electrochemical cell. These compounds contain Oxygen and at least two other elements, which are often transition metals. [31]
These materials offer a wide variety of magnetic and electronic properties, such as: ferromagnetism, ferroelectricity and high-temperature superconductivity.
For the sake of the research complex oxides are used as electrolytes, anodes and cathodes of the fuel cells. [8]
The electronic arrangement deriving from their structure lies between ionic and free-electrons materials: meaning that they are overall neutrally charged and present a crystalline structure when solid. [18] [13]

2.2 Strontium titanate (STO)

In this research Strontium titanate ($SrTiO_3$), which is a single crystal with orientation (100) has only been used as the foundation substrate which provides a proper lattice match for Samarium doped Ceria ($Ce_{0.8}Sm_{0.2}O_{2-\delta}$), inducing an epitaxial growth of the mono crystalline film. [25]

STO belongs to the abundant and prominent Perovskytes Oxides structural family. Such category refers to any material with a crystal structure following the general formula ABO_3, where A is a large radius cation and B a smaller radius cation.
This crystalline structure is called Body Centered Cubic (BCC). In this configuration atoms are arranged at the corners of each cube face of the cell with one at the center of each face, as we can clearly see in a general preview from figure 2.1, and in particular for STO from Fig. 2.2. [32].

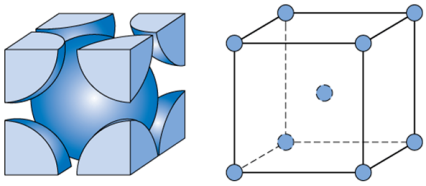

Figure 2.1: Body Centered Cubic crystalline structure

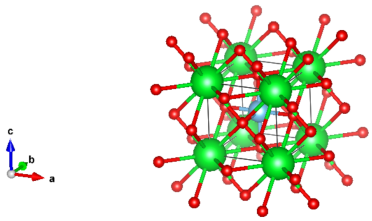

Figure 2.2: STO structure where: green atoms represent Ti, red atoms represent O_3 and the central blue atom represents Sr

2.3 Sacrificial Salt layer (SAO)

A "Sacrificial" Salt layer ($Sr_3Al_2O_6$) is deposited on top of the STO substrate in order to prepare it from the SDC plum that will form on the final deposition as Fig. 2.3 shows. [16]

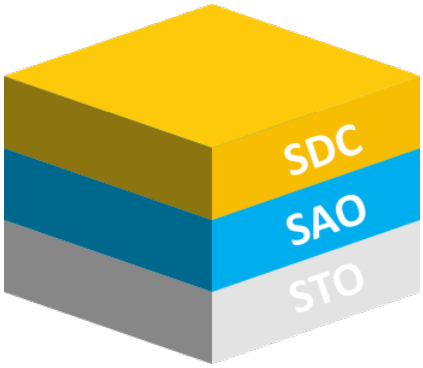

Figure 2.3: Schematic view of the three layers that have been deposited.

The term "Sacrificial" is introduced because this layer, being a salt, dissolves in water in the final stage of the process; detaching the SDC thin film from the STO substrate. An illustration of the operation is shown in Fig. 2.4

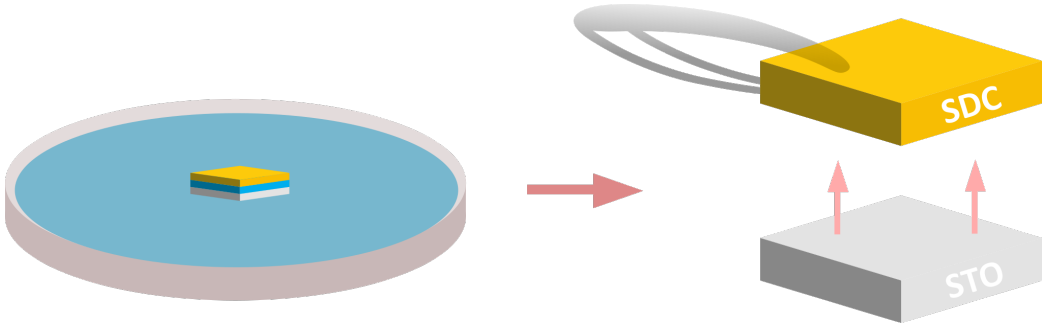

Figure 2.4:
On the left: sample submerged in water and left for several hours into a sealed petri dish in order to dissolve the sacrificial layer.
On the right: SDC film detached from STO using tweezers.

The reason this process is relevant is due to the importance of a good film deposition on a single crystal (such as STO) and the later removal of the latter, to transfer it onto a more complex device made of different parts based on silicon by micro machining techniques. A general chip example is shown in Fig. 2.5

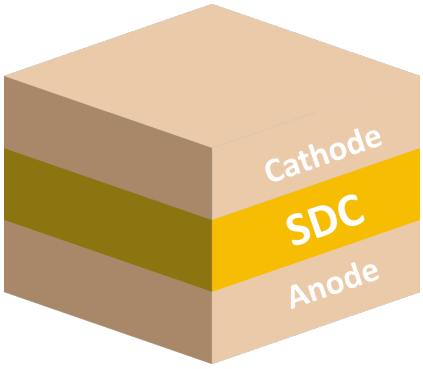

Figure 2.5: General schematic representation of a micro fuel cell, consisting on the SDC thin film used as electrolyte between a cathode and and anode. Note: on the other side of both the anode and the cathode it's often present an interconnect that enables the connection of more cells one to another.

2.4 Samarium Doped Ceria (SDC)

Samarium Doped Ceria consists in dope Ceria (CeO_2) where Cerium cations under certain reducing conditions undergo reduction from Ce^{4+} to Ce^{3+}. [24] [23] [22] This results in an excess of electrons predominantly localized around Ce ions, hence in an n-type semiconductor. When Ceria is Doped with Samarium (CeO_2/Sm) it presents an incredible attitude at being an ionic conductor, due to the production of Oxygen vacancies in the crystal lattice.
In particular the concentration of these vacancies can be expressed following the Kröger–Vink notation [21]:

$$\frac{1}{2}O_2 + 2Ce'_{Ce} + V_O^{\bullet\bullet} \Leftrightarrow 2Ce_{Ce}^X + O_O^X \tag{2.1}$$

- $V_O^{\bullet\bullet}$ is a double positively charged oxide ion vacancy.
- O_O^X is the neutrally charged Oxygen present in the lattice.
- Ce'_{Ce} is a Ce^{+3} cation, i.e. a negatively charged Ce atom
- Ce_{Ce}^X is a Ce^{+4} cation, i.e. a neutrally charged Ce atom

SDC with its fluorite structure presents, differently from STO, a Face Centered Cubic (FCC) crystalline structure. In such a configurations atoms are arranged at the corners and center of each cube face of the cell as we may observe in general FCC preview from Fig. 2.6, and in particular for SDC from Fig. 2.7

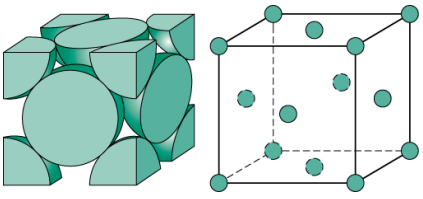

Figure 2.6: Face Centered Cubic crystalline structure.

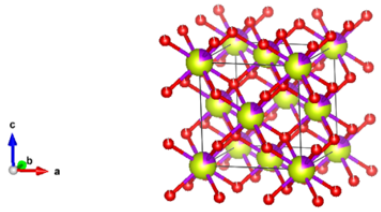

Figure 2.7: SDC structure where: partially yellow and pink atoms represent Ce/Sm and red atoms represent O.

2.5 Why Samarium doped Ceria?

Cerium oxide is the most thoroughly investigated material for the application in solid oxide fuel cells (SOFCs) working in the intermediate-temperature range (500–700°C) [12].
This is because of its pronounced catalytic properties and substantial oxygen-ion conductivity. [30] The high catalytic activity in Ceria is associated with the presence of Ce^{4+}/Ce^{3+} redox couple which is a key to improve the electrochemical properties of the electrodes. Oxygen-ion conduction in Ceria is mediated through a vacancy diffusion mechanism. In oxidizing atmospheres, pure CeO_2 does not have any oxygen vacancy defects and as a result, pure CeO_2 itself is a poor oxygen-ion conductor. [14]
The oxygen vacancy defects are introduced into the CeO_2 structure by partially substituting Ce^{4+} with acceptor cations inside the lattice. Kröger–Vink notation 2.1 expresses this defect reaction.

A note of remark must be made for the remarkable carbon-deposition suppression capability: in fact the electrochemical reduction of CO_2 to CO on the Ceria surface can be written as follows:

$$CO_{2(g)} + 2e^{'} + V_0^{\bullet\bullet} \Leftrightarrow CO_{(g)} + O_O^X + 2Ce_{Ce}^X \tag{2.2}$$

A similar reaction also holds for the water-splitting reaction. The process shown by 2.2 can be summarized in 3 steps:

1. Transport of charge carriers from the bulk to the surface.
2. Adsorption/dissociation of gaseous reactants.
3. Charge transfer at the surface/gas interface.

Deposition systems and analysis techniques

3.1 Pulsed Laser Deposition(PLD)

Pulsed Laser Deposition (PLD) is a physical vapor deposition excellent and simple among all thin film growth techniques because of its capability of reproducing the target composition onto the film substrates.
A high power laser is used inside a vacuum chamber as an external energy source to vaporize a target of the material we want to deposit.
A set of optical and movable components are used to focus the laser beam on the target.
When the laser radiation is absorbed by the target, electromagnetic energy is converted in other forms to vaporize it, forming a plasma plume which is deposited as a thin film forming the different substrates of our specimen. [7]

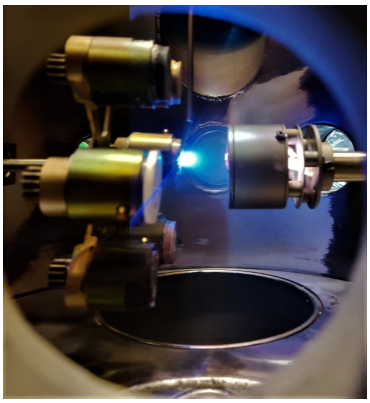

Figure 3.1: Photo of the vacuum chamber. On the left the multi-target rotating holder is positioned. Between the holder and the heater the plume stands out, directed to the substrate positioned on the heater (right)

3.2 Reflection High Energy Electron Diffraction (RHEED) technique

Reflection High Energy Electron Diffraction (RHEED) has assumed modern importance because of its compatibility with the methods of vapor deposition used for the epitaxial growth of thin films. [15]
This technique is used for surface structural analysis and it is incredibly easy to install. A RHEED structure implementation is shown in the following graphical representation. (Fig. 3.2)

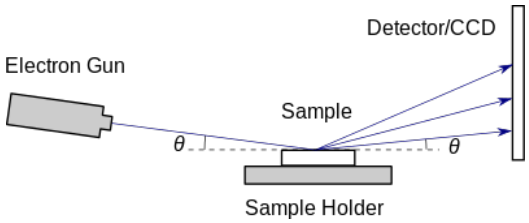

Figure 3.2: Graphical representation of a RHEED structure: an electron gun generates a beam of electrons which strike the sample at a very small angle relative to the sample surface. Incident electrons diffract from surface atoms, and a small fraction of them interfere constructively at specific angles and form regular patterns on the detector. These patterns may be seen in Fig. 3.5

From the arrangement, intensity and profile of the diffraction spots in RHEED patterns, one can obtain various kinds of information;

- Periodicity of the atomic arrangement.
- Flatness of surfaces.
- Epitaxial relation between the grown films/dots with respect to the substrate.
- Grain sizes and general growth mechanism of thin films.
- Numbers of atomic layers grown.

Furthermore, the electrons interfere according to the position of atoms on the sample surface, so the diffraction pattern at the detector is a function of the sample surface.
A schematic representation of the latter can be clearly seen in Fig. 3.3 [3] [11]

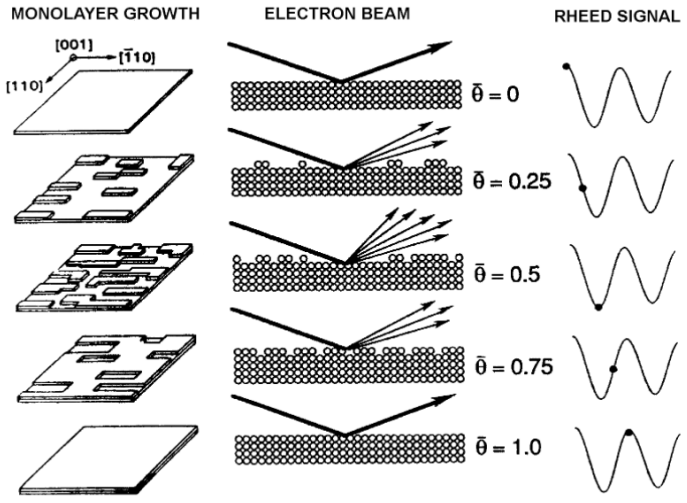

Figure 3.3: RHEED signal depending on the monolayer film growth: signal intensity ("RHEED signal" in the image) is closely interlaced to how much the beam has been scattered after hitting the surface.

3.3 Practical aspects of the method: RHEED patterns

Investigation of the RHEED pattern gives a concrete and tangible idea of what the surface looks like. [9]
For example when the sample has an atomically flat surface and a perfect single-crystalline structure the RHEED pattern will look like Fig. 3.4a : showing a few spots on the detector screen.
As shown in Fig. 3.4b instead, when the surface is flat but presents different small domains, the detector screen will show some streaks due to a slightly different electron diffraction. Finally, as seen in Fig. 3.4c, when 3D single crystals (or islands) are formed, the screen will depict instead several spots.

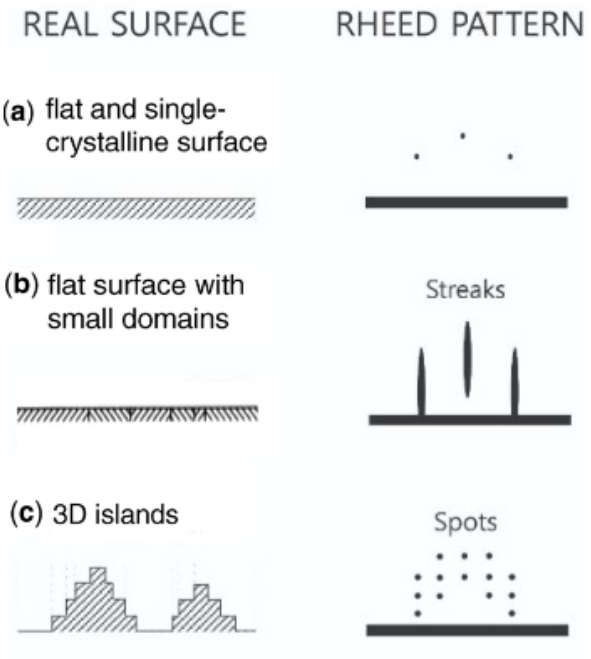

Figure 3.4: Schematics of various kinds of real surfaces and their RHEED patterns (courtesy by Yoshimi Horio).

The pattern analysis has been carried out for all of the three various depositions and the results are right as expected.
As can be seen from Fig. 3.5a, the STO substrate presents the same structure as the previously discussed "Flat and single-crystalline structure".

Notice: it is somewhat clear that the actual images will be slightly different from the ideal case, presenting some noise and imperfections.

From Fig 3.5b the streaks are clearly evident, representing the sacrificial layer deposition which, although being flat, presents different domains. Moreover from Fig. 3.5c the several transmission points appear on the detector screen, representing the well grown SDC island. Most importantly instead, from Fig. 3.5d the tendency of those dots to become streaks represents the islands levelling out, resulting in a flat surface with small domains.

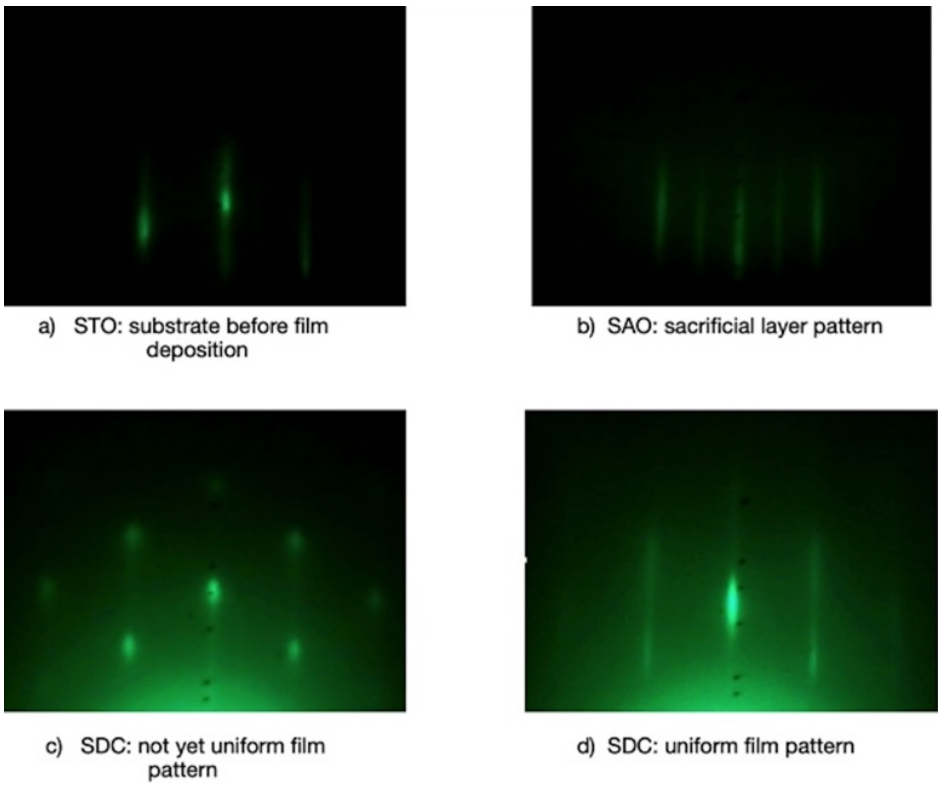

Figure 3.5: Picture taken from a camera standing right above the RHEED detector, representing the 4 different patterns created by the diffracted electrons.

3.4 X-Ray diffraction(XRD) technique

In the X-Ray diffraction, the sample is placed in the center of an instrument and illuminated with a beam of X-Rays.

The X-Ray tube and detector generally move in a synchronised motion, unless the sample investigated is a single crystal: in which case the latter would be the one rotating until the peak with greatest diffracted intensity is found. The signal coming from the sample is then recorded and plotted in an intensity-2θ graph where the peaks are observed, related to the atomic structure of the sample.

The basis of diffraction analysis is the interference between incident and diffracted wave.[10] Such interference can be either constructive (i.e. superposition of waves) when the phase shift is a multiple of 2π, or destructive in accordance with **Bragg's law**:

$$n\lambda = 2d_{hkl}sin\theta$$

- n is a positive integer representing the harmonic order of the diffraction.
- λ is the wavelength of the electromagnetic radiation which can have similar dimensions with the distances between planes within the crystal's lattice d_{hkl}: these correspond to X-Rays.
- d is the spacing between adjacent planes in the atomic lattice, as Fig. 3.7 shows.
- hkl are the Miller indices: a set of three integers that constitute a notation system for the identification of directions and planes within the crystals. Some further graphical representation is is shown in Fig. 3.6
- θ is the angle between the diffracted ray and the scattering plane. Only for given a λ specific angles θ give rise to diffraction: this represents the unique signature of a crystalline structure.

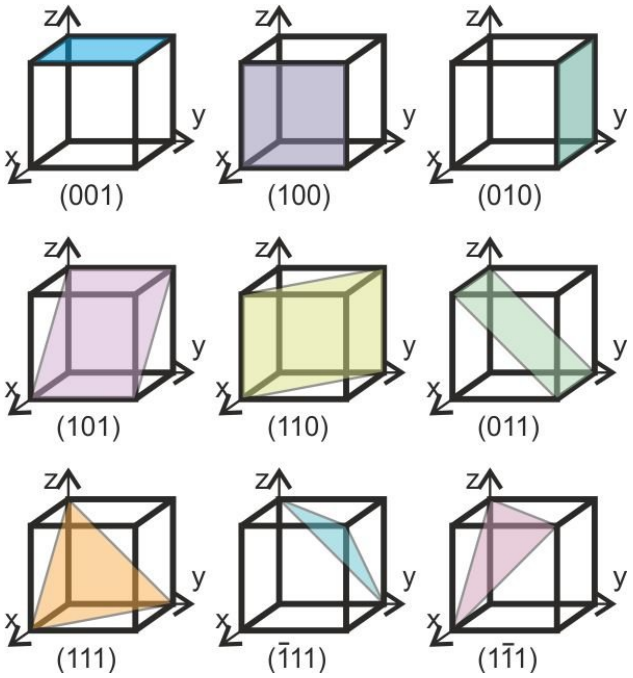

Figure 3.6: Graphical representation of the fundamental combinations of the three Miller indices: different multiples and sub-multiples of these combinations may be defined accordingly.

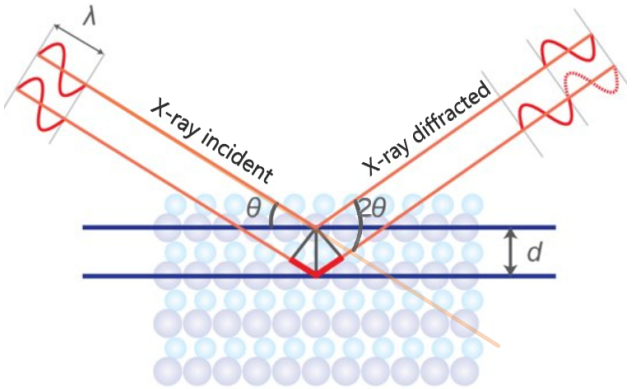

Figure 3.7: Illustration of Bragg's most important parameters. Incidents X-Rays with a wavelength equal to λ hit the electrons of the atom lattice at an angle θ causing an elastic scattering of different waves. Some of those waves will be diffracted and interact constructively, in accordance with Bragg's law, increasing the intensity at an angle 2θ.

3.5 XRD experiment and analysis

The experiment is carried out by placing the sample in the sample holder in the center of the goniometer. and by modifying the beam size depending on the sample width: slits with different sizes are used to do so. Bigger slits are supposed to be used for bigger objects and a rough overall estimations, whereas smaller slits are supposed to be used for accuracy and precision. [6]

After this setup, the acquisition parameters must be chosen, some of the most important being the starting angle, the final angle, the step etc.
Once this has been done, a first analysis is executed and the peaks coming from the diffraction pattern of the 2θ scan are found. Now that the peaks are identified, a narrower scan range is chosen around specific peaks using a smaller step size in angle to obtain a higher resolution pattern. After that, the data can be finally analyzed to study the structure of the material. [4]

The previously defined process for the XRD analysis of single crystals is known as the Rocking Curve (RC).
By studying the RC it is possible to estimate the film mosaic spread, or in other words: the deposition quality.
In such a procedure the detector is positioned at 2θ Bragg, while the angle between the incident ray and the surface of the sample is moved around the Bragg's angle θ as Fig. 3.8 schematically shows. [29] [24]

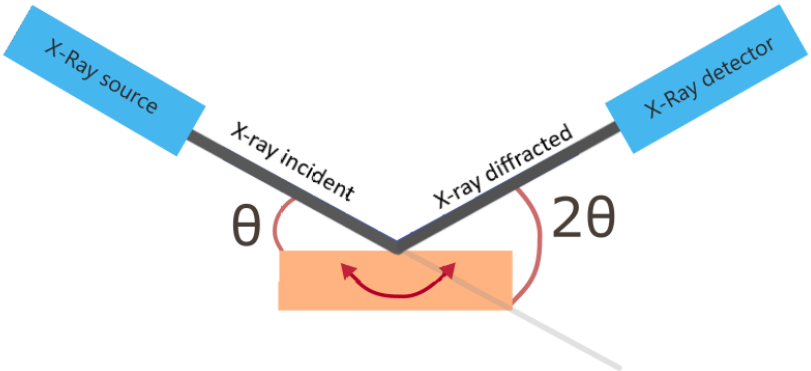

Figure 3.8: Experimental setup conditions of the RC process: the sample is "rocked" from side to side in search for its peak, while the X-ray tube and the X-Ray detector stay in their predefined position of respectively θ and 2θBragg without moving.

The analysis instead is carried out by performing a 2θ scan along with an ω scan of the sample.
The former shows the orientation and the intensity of the different materials studied, whereas the latter shows the mosaic spread of the film, or in other words: its crystallographic qualities.

Fig. 3.9 shows the different diffraction patterns, or more precisely, from left to right of each row respectively: the 2θ scan, the ω scan and a graphical illustration of the film studied.
In particular:

- Fig. 3.9(a,b,c) show the SDC deposition onto the STO substrate: SDC has a (002) orientation with a mosaic spread (FWHM) of 0.7° at its bragg angle, resulting in an overall good crystallographic quality of the film.

- Fig. 3.9(d,e,f) show the SDC deposition with the use of a SAO buffer layer: SDC and STO have similar peaks, SDC orientation is again (002) with a remarkable mosaic spread of 0.4° at its bragg angle.

- Fig. 3.9(g,h,i) show the SDC thin film free standing attached to the polymer membrane after being detached from the substrate, thanks to the sacrificial layer. SDC keeps the (002) orientation however the mosaic spread increases to 1.5° because the polymer doesn't have a perfectly smooth surface.

- Fig. 3.9l to Fig.3.9n show the SDC finally transferred to an Si layer completely undamaged. SDC orientations is clearly unchanged and the mosaic spread decreases again to 0.68°: remarking the good film quality.

In conclusion, as the XRD proves, the film keeps a remarkable mosaic spread after being transferred to the Si layer, which is exactly the aim of the XRD analysis as well as the desired result.

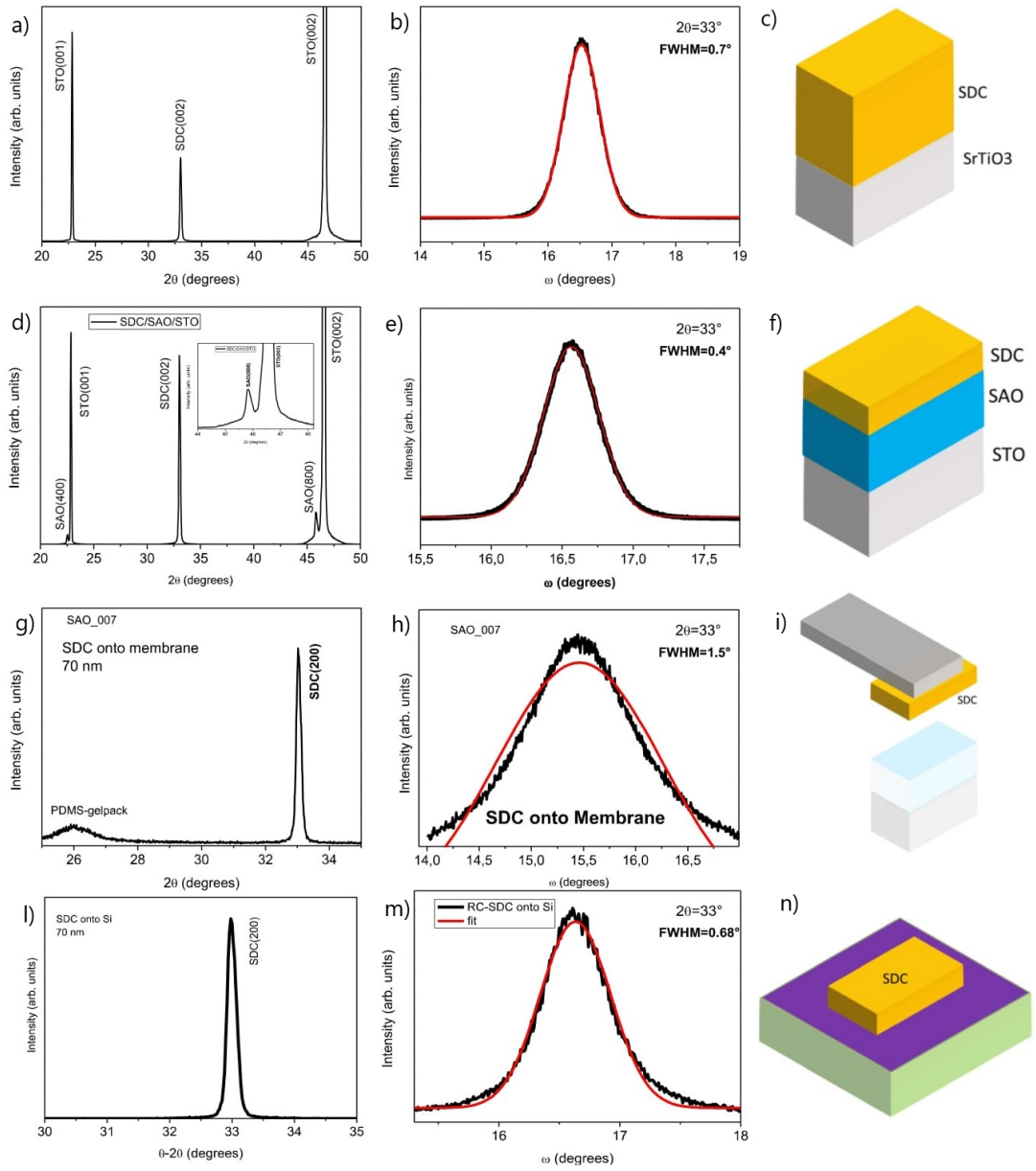

Figure 3.9: The first two plots of each row show respectively the 2θ scan and the ω scan of the film in different configurations, whereas the last figure is a graphical representation of the film configuration analyzed.
Note how after SDC has been detached from STO thanks to the SAO in Fig. 3.9i , it remains undamaged while also keeping a great FWHM up to the final transfer to the Si layer (Fig. 3.9n)

Conclusions

This thesis aim was to report and spread light on the latest state-of-the-art technology that might give rise to an important green energy improvement in our daily life. An overview on fuel cells and on already present SOFC/SOEC, along with the newly developing micro-SOFC has thus been given.
This work was especially focused on Complex Oxides growth in thin film shape by Pulsed Laser Deposition technique. It's been shown how such a technique is incredibly efficient for epitaxial growth of thin films, and how can the RHEED analysis represent a great match for such a technique. In particular the attention was directed towards the most promising complex oxides materials, such as: STO (perovskyte used as foundation layer), SAO (salt used as sacrificial layer) and SDC (fluorite used as electrolyte). The crystalline structure of perovskytes and fluorites has been investigated. It's been studied how important it is to find a good candidate as buffer layer match to guarantee SDC epitaxial growth by using buffer layers such as the STO perovskyte, but also how such a layer is important in later analysis due to its capability of not influencing the SDC analysis. Finally, the samples have been studied by XRD-analysis means both under the $\theta - 2\theta$ perspective and the ω scan to investigate the crystalline disorder at different stages.

Acknowledgments

Throughout this journey I have received a great deal of support and assistance and i would hence like to show my appreciation to those who have helped me get here.

I would first and foremost like to thank my supervisor, Professor Simone Senna, whose incredible expertise in the field was invaluable to my training. Your way of attending to your students needs and questions is remarkable. Thank you for all the material you provided and handed me. Finally, thanks for your insightful feedbacks which brought my thinking process and my work to an higher level.

I would like to acknowledge both Professor Antonello Tebano and Dr. Daniele Di Castro along with the Pulsed Laser Deposition research group for always being there to clarify my doubts and being part of my growth process.

I would also like to thank my colleagues for helping me throughout the ups and downs of the academic life and providing me a happy distraction to ease my mind outside work. Special thanks goes to one of the most self-driven men i have had the pleasure to meet so far. Thanks Mohammadreza Tohidi.

In addition i would like to thank my cousin Jonathan Di Biase, who helped me both academically and mentally wise.
Finally my most special thank goes to my sweet girlfriend Alice for always lending and ear when necessary, for supporting me and for providing me with stimulating discussions from both my field and her field.
Thank you from the bottom of my heart.

Nikolas Vitaliti

Bibliography

[1] Jong Dae Baek, Kang-Yu Liu, and Pei-Chen Su. A functional micro-solid oxide fuel cell with a 10 nm-thick freestanding electrolyte. *Journal of Materials Chemistry A*, 5(35):18414–18419, 2017.

[2] A Ballantine. Everything you need to know about solid oxide fuel cells. *Bloom Energy*, 2019.

[3] Wolfgang Braun. *Applied RHEED: reflection high-energy electron diffraction during crystal growth*, volume 154. Springer Science & Business Media, 1999.

[4] Cambridge. X-ray diffraction. *Ingegneria dei materiali*, 2022.

[5] Steven G Chalk and James F Miller. Key challenges and recent progress in batteries, fuel cells, and hydrogen storage for clean energy systems. *Journal of Power Sources*, 159(1):73–80, 2006.

[6] Ashish Chauhan and Priyanka Chauhan. Powder xrd technique and its applications in science and technology. *J Anal Bioanal Tech*, 5(5):1–5, 2014.

[7] Douglas B Chrisey, Graham K Hubler, et al. Pulsed laser deposition of thin films. 1994.

[8] Wikipedia contributors. Complex oxides, 2020.

[9] M Dabrowska-Szata. Analysis of rheed pattern from semiconductor surfaces. *Materials chemistry and physics*, 81(2-3):257–259, 2003.

[10] J Epp. X-ray diffraction (xrd) techniques for materials characterization. In *Materials characterization using nondestructive evaluation (NDE) methods*, pages 81–124. Elsevier, 2016.

[11] Ayahiko Ichimiya, Philip I Cohen, and Philip I Cohen. *Reflection high-energy electron diffraction*. Cambridge University Press, 2004.

[12] Hideaki Inaba and Hiroaki Tagawa. Ceria-based solid electrolytes. *Solid state ionics*, 83(1-2):1–16, 1996.

[13] Charles Kittel. Introduction to solid state physics, john wiley & sons. *Inc., Sixth edition,(New York, 1986)*, 2005.

[14] Julius Koettgen, Steffen Grieshammer, Philipp Hein, Benjamin OH Grope, Masanobu Nakayama, and Manfred Martin. Understanding the ionic conductivity maximum in doped ceria: trapping and blocking. *Physical Chemistry Chemical Physics*, 20(21):14291–14321, 2018.

[15] Łukasz Kokosza, Jakub Pawlak, Zbigniew Mitura, and Marek Przybylski. Simplified determination of rheed patterns and its explanation shown with the use of 3d computer graphics. *Materials*, 14(11):3056, 2021.

[16] Di Lu, David J Baek, Seung Sae Hong, Lena F Kourkoutis, Yasuyuki Hikita, and Harold Y Hwang. Synthesis of freestanding single-crystal perovskite films and heterostructures by etching of sacrificial water-soluble layers. *Nature materials*, 15(12):1255–1260, 2016.

[17] Umberto Lucia. Overview on fuel cells. *Renewable and Sustainable Energy Reviews*, 30:164–169, 2014.

[18] D Meyers, Jian Liu, JW Freeland, S Middey, M Kareev, Jihwan Kwon, JM Zuo, Yi-De Chuang, JW Kim, PJ Ryan, et al. Pure electronic metal-insulator transition at the interface of complex oxides. *Scientific reports*, 6(1):1–8, 2016.

[19] A Nafees and Ruwaida Abdul Rasid. Study of natural gas powered solid oxide fuel cell simulation and modeling. *IOP Conference Series: Materials Science and Engineering*, 702:012017, 12 2019.

[20] Aziz Nechache and Stéphane Hody. Alternative and innovative solid oxide electrolysis cell materials: A short review. *Renewable and Sustainable Energy Reviews*, 149:111322, 2021.

[21] Truls Norby. A kr öger-vink compatible notation for defects in inherently defective sublattices. *Journal of the Korean Ceramic Society*, 47(1):19–25, 2010.

[22] Simone Sanna. Thin films growth by pulsed laser deposition for solid oxide fuel cell applications. 2010.

[23] Simone Sanna, Vincenzo Esposito, Jens Wenzel Andreasen, Johan Hjelm, Wei Zhang, Takeshi Kasama, Søren Bredmose Simonsen, Mogens Christensen, Søren Linderoth, and Nini Pryds. Enhancement of the chemical stability in confined δ-bi2o3. *Nature materials*, 14(5):500–504, 2015.

[24] Simone Sanna, Vincenzo Esposito, Daniele Pergolesi, Andrea Orsini, Antonello Tebano, Silvia Licoccia, Giuseppe Balestrino, and Enrico Traversa. Fabrication and electrochemical properties of epitaxial samarium-doped ceria films on srtio3-buffered mgo substrates. *Advanced Functional Materials*, 19(11):1713–1719, 2009.

[25] Simone Sanna, Vincenzo Esposito, Antonello Tebano, Silvia Licoccia, Enrico Traversa, and Giuseppe Balestrino. Enhancement of ionic conductivity in sm-doped ceria/yttria-stabilized zirconia heteroepitaxial structures. *Small*, 6(17):1863–1867, 2010.

[26] Subhash C Singhal. Advances in solid oxide fuel cell technology. *Solid state ionics*, 135(1-4):305–313, 2000.

[27] Javad Soltanzadeh and Reza Salami. Role of public r&d funding in fuel cell: analysis on iranian universities. *International Journal of Energy Technology and Policy*, 14:409, 01 2018.

[28] Toshiba Energy Systems & Solutions. Low-carbon society of next generation. *https://www.global.toshiba/ww/products-solutions/hydrogen/research.html*, 2022.

[29] VS Speriosu and Thad Vreeland Jr. X-ray rocking curve analysis of superlattices. *Journal of applied physics*, 56(6):1591–1600, 1984.

[30] Brian CH Steele. Appraisal of ce1- ygdyo2- y/2 electrolytes for it-sofc operation at 500° c. *Solid state ionics*, 129(1-4):95–110, 2000.

[31] Douglas J Buttrey Thomas Vogt. *Complex Oxides: An Introduction*. world scientific.

[32] Kenji Uchino, Shoichiro Nomura, Leslie E Cross, Robert E Newnham, and Sei J Jang. Electrostrictive effect in perovskites and its transducer applications. *Journal of Materials science*, 16(3):569–578, 1981.

[33] Osamu Yamamoto. Solid oxide fuel cells: fundamental aspects and prospects. *Electrochimica Acta*, 45(15-16):2423–2435, 2000.